Machine Learning–Guided Stochastic Switching Modeling of Chronic Kidney Disease

Amina Allali[1], Karima Moumane[1(✉)], and Saida Amine[2]

[1] Software Project Management Research Team, ENSIAS, Mohammed V University in Rabat, Rabat, Morocco
aminaallali86@gmail.com , karima.moumane@ensias.um5.ac.ma

[2] Department of Mathematics and application, Faculty of Sciences and Technology, Hassan II University of Casablanca, PO Box 146, 20650 Mohammedia, Morocco
aminesaida52@gmail.com

Abstract. This study develops a machine learning–guided stochastic switching model to analyze the progression of chronic kidney disease (CKD) under personalized treatment strategies. The main objective is to understand how treatment switching under uncertainty influences disease evolution and to identify conditions under which CKD progression can be controlled. Clinical data are used to estimate model parameters through machine learning techniques, enabling a patient-specific and data-driven representation of disease dynamics. The proposed framework combines deterministic and stochastic analyses to capture both baseline disease behavior and random perturbations in treatment response. Theoretical results establish the existence, uniqueness, and positivity of solutions, ensuring biological feasibility. Stability analysis of the deterministic model identifies disease-free and endemic equilibria and associated threshold parameters. For the stochastic model, Lyapunov-based methods are used to derive conditions for extinction and persistence of the disease. Numerical simulations based on real clinical data validate the theoretical findings and demonstrate the impact of different treatment strategies on CKD progression. Overall, the study highlights the relevance of integrating machine learning with stochastic modeling to support personalized and data-driven management of chronic kidney disease.

Keywords: Chronic Kidney Disease (CKD) · Mathematical Modeling · Stochastic Switching · Personalized Treatment · Data-Driven Modeling · Machine Learning · Numerical simulations

1 Introduction

Chronic Kidney Disease (CKD) is a progressive and irreversible disorder that represents a major global public health challenge, affecting hundreds of millions of individuals worldwide [1]. The disease is characterized by a gradual loss of

© The Author(s), under exclusive license to Springer Nature Switzerland AG 2027
O. Gervasi et al. (Eds.): ICCSA 2026, LNCS 16768, pp. 511–531, 2027.
https://doi.org/10.1007/978-3-032-30488-9_32

functional nephrons, persistent inflammatory processes, excessive renal fibrosis, and a continuous decline in the glomerular filtration rate (GFR). If left untreated, CKD may progress to end-stage renal disease, requiring dialysis or kidney transplantation, and is associated with high morbidity and mortality rates [25]. Due to its complex and multifactorial nature, CKD progression exhibits substantial inter-individual variability, posing significant challenges for clinical management and therapeutic decision-making.

Mathematical modeling has proven to be a powerful tool for understanding the temporal dynamics of chronic diseases and for evaluating therapeutic strategies. Deterministic compartmental models have been widely used to describe the interactions between inflammation, fibrosis, nephron loss, and renal function decline in CKD [18,23]. These models enable qualitative analysis of equilibrium states and threshold conditions governing disease stabilization or progression. However, classical deterministic approaches often fail to capture intrinsic biological variability arising from patient heterogeneity, environmental factors, and fluctuating treatment responses.

To address these limitations, stochastic modeling frameworks have been introduced to account for random perturbations in disease dynamics. Stochastic differential equation (SDE) models incorporate environmental and physiological uncertainties and provide a more realistic representation of biological systems [9,11,13,15]. In biomedical applications, stochasticity may significantly alter system behavior, potentially leading to disease extinction in scenarios where deterministic models predict persistence [3,4]. Such models are commonly driven by Brownian motion or Gaussian white noise and have been successfully applied in epidemiology and chronic disease modeling [21].

In parallel, the increasing availability of clinical datasets has stimulated the integration of machine learning techniques into biomedical modeling. Machine learning methods have demonstrated strong potential for parameter estimation, prediction, and pattern discovery in high-dimensional clinical data [2,7,10,14,17,22]. In the context of CKD, data-driven approaches enable the calibration of mechanistic models using real patient data and facilitate the design of personalized treatment strategies. The combination of machine learning with mechanistic stochastic models provides a powerful framework for bridging theoretical analysis and clinical relevance. Compared to previous studies on chronic kidney disease modeling, which mainly focus on either deterministic frameworks or stochastic dynamics separately [3,23], this work integrates both approaches within a machine learning–guided stochastic switching framework to better capture patient-specific variability and treatment adaptation.

Motivated by these developments, this study proposes a machine learning–guided stochastic switching model for Chronic Kidney Disease under personalized treatment strategies. The model combines deterministic and stochastic dynamics to describe the temporal evolution of functional nephron population, renal fibrosis, inflammatory activity, renal function, and treatment intensity. A switching treatment mechanism is incorporated to reflect intermittent or adaptive therapeutic protocols commonly observed in clinical practice. Model param-

eters are estimated using real clinical datasets, and the calibrated model is validated through numerical simulations.

The main contributions of this work are summarized as follows:

- A novel deterministic and stochastic CKD model incorporating treatment switching is formulated.
- Existence, uniqueness, positivity, and boundedness of solutions are established.
- Extinction and persistence conditions are derived using Lyapunov function techniques and LaSalle's invariance principle [5, 12, 16, 26].
- Machine learning methods are employed for parameter estimation from real clinical data.
- Numerical simulations are conducted to validate the analytical results and assess therapy optimization.

The remainder of this manuscript is organized as follows. Section 2 presents the model formulation along with its biological interpretation. Section 3 is devoted to the deterministic analysis. Section 4 introduces the stochastic switching model and establishes the existence, uniqueness, and positivity of solutions, as well as extinction and persistence in mean results. Section 5 presents numerical simulations and data-driven validation. Finally, Sect. 6 concludes the paper with a summary of the main findings and perspectives for future research.

2 Formulation of the Models

Let t represent the time, and $N(t)$ represents the fraction of functional nephrons, where $F(t)$ denotes the level of renal fibrosis, $I(t)$ represents the intensity of chronic inflammation affecting the kidneys, $G(t)$ denotes the normalized glomerular filtration rate (GFR), and $T(t)$ represents the cumulative therapeutic effect applied to the patient. Based on the pathophysiological dynamics of chronic kidney disease (CKD), we assume nonlinear interaction rates governing disease progression. Functional nephrons decline due to fibrosis and inflammation effects at the rates $\alpha_1 F(t)N(t)$ and $\alpha_2(T)I(t)N(t)$, respectively, where α_1 denotes the fibrosis–induced nephron loss rate and $\alpha_2(T)$ represents inflammation–induced nephron damage modulated by treatment. Fibrosis progresses due to inflammatory activity at the rate $\beta_1(T)I(t)(1-F(t))$, where $\beta_1(T)$ denotes the treatment–dependent fibrosis progression rate, while μ represents the natural fibrosis resolution rate. Inflammation increases due to aggregated clinical risk factors at the rate ηH and fibrosis feedback at the rate $\kappa F(t)$, where η denotes the inflammation induction rate and κ represents fibrosis–driven inflammatory amplification. Inflammation resolves at the treatment–enhanced rate $\delta(T)I(t)$. The glomerular filtration rate improves proportionally to functional nephron mass at the rate $\rho N(t)$, where ρ denotes nephron contribution to renal function, and declines due to fibrosis damage at the rate $\gamma F(t)G(t)$. Treatment effect accumulates according to the therapeutic control input $u(t)$ and decays over time at the rate $\omega T(t)$. All parameters are described in Table 1 while the governing equations describing

transitions in the model are given in Eq. (1). Besides, the following assumptions were taken into consideration while formulating the model:

A_1 : All the initial state variables are non–negative, that is $N(0), F(0), I(0), G(0), T(0) \geq 0$.
A_2 : Model variables and parameters are all non–negative.
A_3 : Functional nephron loss is driven by both fibrosis and inflammation.
A_4 : Fibrosis progression is induced by inflammatory processes and saturates at a maximal biological level.
A_5 : Inflammation is induced by clinical risk factors and fibrosis feedback.
A_6 : Treatment reduces inflammation and fibrosis progression.
A_7 : Treatment improves nephron preservation and renal function.
A_8 : The therapeutic effect decays naturally over time.
A_9 : Glomerular filtration rate depends positively on functional nephron mass.
A_{10} : Fibrosis contributes negatively to renal filtration capacity.

Considering other features of CKD progression and the above assumptions (A_1–A_{10}), the system can be represented by the following differential equations:

$$\begin{cases} \dfrac{dN(t)}{dt} = -\alpha_1 F(t)N(t) - \alpha_2(T)I(t)N(t), \\ \dfrac{dF(t)}{dt} = \beta_1(T)I(t)(1-F(t)) - \mu F(t), \\ \dfrac{dI(t)}{dt} = \eta H + \kappa F(t) - \delta(T)I(t), \\ \dfrac{dG(t)}{dt} = \rho N(t) - \gamma F(t)G(t), \\ \dfrac{dT(t)}{dt} = u(t) - \omega T(t). \end{cases} \tag{1}$$

The treatment–modulated parameters are defined as:

$$\alpha_2(T) = \alpha_2^0(1-\xi T), \qquad \beta_1(T) = \beta_1^0(1-\theta T), \qquad \delta(T) = \delta_0 + \delta_1 T.$$

Since, in real situations, the temporal dynamics of chronic kidney disease are inevitably influenced by random factors, we consider here stochastic perturbations proportional to the population sizes $N(t), F(t), I(t), G(t)$, and the treatment level $T(t)$. To obtain the stochastic version of the deterministic model, we introduce multiplicative noise into the system 1. Therefore, the stochastic version of the CKD model with treatment and switching can be formulated as the following system of stochastic differential equations:

$$\begin{cases} dN(t) = \big[-\alpha_1^{r(t)} FN - \alpha_2^{r(t)}(T)IN\big]dt + \sigma_1^{r(t)} N\, dB_1(t), \\ dF(t) = \big[\beta_1^{r(t)}(T)I(1-F) - \mu^{r(t)}F\big]dt + \sigma_2^{r(t)} F\, dB_2(t), \\ dI(t) = \big[\eta^{r(t)}H + \kappa^{r(t)}F - \delta^{r(t)}(T)I\big]dt + \sigma_3^{r(t)} I\, dB_3(t), \\ dG(t) = \big[\rho^{r(t)}N - \gamma^{r(t)}FG\big]dt + \sigma_4^{r(t)} G\, dB_4(t), \\ dT(t) = \big[u^{r(t)}(t) - \omega^{r(t)}T\big]dt + \sigma_5^{r(t)} T\, dB_5(t), \end{cases} \tag{2}$$

Table 1. Model parameters and variables

Notion	Meaning
α_1	Fibrosis–induced nephron loss rate
$\alpha_2(T)$	Inflammation–induced nephron loss rate
$\beta_1(T)$	Fibrosis progression rate
μ	Natural fibrosis resolution rate
η	Risk factor–induced inflammation rate
κ	Fibrosis feedback on inflammation
$\delta(T)$	Inflammation resolution rate
ρ	Nephron contribution to GFR
γ	Fibrosis impact on GFR
ω	Treatment decay rate
$u(t)$	Treatment control input
H	Aggregate risk factor level

where $B_i(t)$, for $i = 1, \cdots, 5$, represent independent standard Brownian motions, and $\sigma_i^{r(t)2} > 0$, $i = 1, \cdots, 5$, denote the intensities of the Gaussian noises. The superscript $r(t)$ indicates that the parameters switch according to the current disease progression regime, modeled as a continuous-time Markov chain. In the context of our CKD model, the stochastic terms $\sigma_1^{r(t)} N(t) dB_1(t)$, $\sigma_2^{r(t)} F(t) dB_2(t)$, $\sigma_3^{r(t)} I(t) dB_3(t)$, $\sigma_4^{r(t)} G(t) dB_4(t)$, and $\sigma_5^{r(t)} T(t) dB_5(t)$ biologically reflect random fluctuations in disease progression, fibrosis development, inflammation, kidney function, and treatment response, including variations due to patient-specific factors and environmental influences.

In this section, we have stated the main assumptions regarding CKD progression, fibrosis, inflammation, kidney function, and treatment response. Based on these assumptions, the corresponding mathematical formulation of the model was developed. The deterministic model was then extended into a stochastic model by including multiplicative noise terms. In the next section, the deterministic version of the model will be analyzed to present its dynamical features, including equilibrium points and stability properties.

3 Deterministic Stability of System (1)

In this section, we intend to discuss the analysis of existence, boundedness and uniqueness of a positive solution for the CKD model (1). For this purpose, using the classical theory of ODEs [6,24], we will focus on the conditions which guarantee the global stability of equilibria.

3.1 Existence, Uniqueness and Boundedness of the Positive Solution of System (1)

This subsection studies the existence, boundedness and uniqueness of the non-negative solution to the proposed CKD model (1) with initial non-negative conditions

$$N(0) \geq 0, F(0) \geq 0, I(0) \geq 0, G(0) \geq 0, T(0) \geq 0. \tag{3}$$

Theorem 1. *Under the initial conditions (3), the CKD model (1) possesses a unique global positive solution in* $\mathbb{R}^5_+$. *Moreover, the closed set*

$$\Gamma = \{(N, F, I, G, T) \in \mathbb{R}^5_+ \mid N(t) \leq N_{\max}\}$$

remains positively invariant, where $N_{\max}$ *is an upper bound for the functional nephron fraction.*

Proof: Suppose that at time $t^* > 0$, $N(t^*) = 0$. The first equation of system (1) gives

$$\left.\frac{dN(t)}{dt}\right|_{t^*} = -\alpha_1^{r(t^*)} FN - \alpha_2^{r(t^*)}(T)IN\Big|_{N=0} = 0.$$

Hence $N(t)$ cannot become negative and remains non-negative for all $t \geq 0$, by continuity of solutions. Similarly, the second, third, fourth and fifth equations imply that
$F(t), I(t), G(t), T(t) \geq 0$ for all $t \geq 0$. Thus, all solutions are clearly positive for every $t \geq 0$.
To illustrate the boundedness of the solution, we define

$$X(t) = N(t) + F(t) + I(t) + G(t) + T(t),$$

then

$$\frac{dX}{dt} = \frac{dN}{dt} + \frac{dF}{dt} + \frac{dI}{dt} + \frac{dG}{dt} + \frac{dT}{dt}.$$

Using the system (1) and ignoring the negative interaction terms for an upper estimate, we obtain

$$dX(t) \leq \big[\text{sum of positive input terms} - \min(\alpha_1, \mu, \omega)X(t)\big]dt.$$

By classical comparison theorem for ODEs, it follows that

$$X(t) \leq e^{-\lambda t}\left(X(0) - \frac{\text{sum of input terms}}{\lambda}\right) + \frac{\text{sum of input terms}}{\lambda},$$

where $\lambda = \min(\alpha_1, \mu, \omega)$ is a positive constant. Hence, if $X(0)$ is bounded, then $X(t)$ remains bounded for all $t \geq 0$, and the set Γ is positively invariant. □

3.2 Equilibria and Threshold Parameters of System (1)

In this section, we assume that each variable $N(t), F(t), I(t), G(t)$ and $T(t)$ represents the corresponding fraction of the total functional units at time t. Although the treatment equation is structurally decoupled from the rest of the system, the treatment indirectly influences the dynamics of the biological variables through treatment-dependent parameters, namely $\alpha_2(T)$, $\beta_1(T)$, and $\delta(T)$. Consequently, the system remains fully coupled, and the dynamics of $T(t)$ play an essential role in modulating the progression of inflammation, fibrosis, and nephron loss.

3.2.1 Disease-Free Equilibrium (DFE)

To determine the functional-unit-preserving equilibrium of model (1), we set all right-hand sides equal to zero. The disease-free equilibrium (DFE) is given by

$$E_0^* = (N_0^*, F_0^*, I_0^*, G_0^*, T_0^*) = \left(N_{\max}, 0, 0, \frac{\rho N_{\max}}{\gamma}, \frac{u}{\omega} \right),$$

where $N_{\max}$ denotes the maximal number of functional nephrons in the absence of fibrosis and inflammation, and $T_0^* = \frac{u}{\omega}$ represents the steady-state level of treatment under a constant administration rate u.

3.2.2 Threshold Parameter

To derive the threshold parameter governing disease progression and fibrosis development, we employ the classical next-generation matrix approach [8,19]. Accordingly, the basic reproduction number associated with system(1) is given by

$$\mathcal{R}_0 = \frac{\beta_1(T_0)\, N_0^*}{\mu + \delta(T_0)}. \tag{4}$$

In the context of chronic kidney disease, $\mathcal{R}_0$ does not represent a transmission potential between individuals, but rather quantifies the intrinsic capacity of inflammation to induce fibrosis and promote disease progression within the kidney. Specifically, $\mathcal{R}_0$ compares the fibrosis-inducing effect of inflammation, modulated by treatment through $\beta_1(T_0)$ and the available functional nephron reserve N_0^*, to the overall resolution rate of inflammation and fibrosis, represented by $\mu + \delta(T_0)$.

If $\mathcal{R}_0 < 1$, resolution mechanisms dominate, leading to the attenuation of inflammation and fibrosis and the preservation of renal function. Conversely, if $\mathcal{R}_0 > 1$, fibrotic progression prevails, resulting in sustained inflammation, nephron loss, and deterioration of kidney function despite treatment.

3.2.3 Endemic Equilibrium

The endemic equilibrium $E^* = (N^*, F^*, I^*, G^*, T^*)$ of the chronic kidney disease model is obtained by setting all time derivatives equal to zero. Assuming a constant treatment input $u(t) = u$, the steady-state treatment level is given by

$$T^* = \frac{u}{\omega}.$$

The equilibrium level of inflammation satisfies

$$I^* = \frac{\eta H + \kappa F^*}{\delta(T^*)},$$

while the fibrosis level is determined by the balance between fibrosis progression and natural resolution,

$$F^* = \frac{\beta_1(T^*)I^*}{\mu + \beta_1(T^*)I^*}.$$

The glomerular filtration rate at equilibrium is expressed as

$$G^* = \frac{\rho N^*}{\gamma F^*}.$$

It is important to note that the equation governing the functional nephron population does not yield an explicit algebraic expression for N^*. Instead, N^* remains implicitly determined by the long-term dynamics of the system and the initial renal reserve. Consequently, the endemic equilibrium is characterized by positive steady-state levels of inflammation and fibrosis, corresponding to a persistent chronic disease state.

3.3 Global Stability Analysis

Theorem 2. *If $\mathcal{R}_0 < 1$, the disease-free equilibrium E_0 of system (1) is globally asymptotically stable in the feasible region.*

Proof. Consider the Lyapunov function

$$V_1(F, I) = F + \frac{\mu + \delta(T_0)}{\beta_1(T_0)} I,$$

which is positive definite for all $(F, I) \in \mathbb{R}^2_+$ and vanishes only at the disease-free equilibrium E_0. Taking the time derivative of V along the trajectories of system(1), we obtain

$$\frac{dV_1}{dt} \leq (\mu + \delta(T_0))(\mathcal{R}_0 - 1)I.$$

When $\mathcal{R}_0 < 1$, it follows that $\frac{dV_1}{dt} \leq 0$, with equality if and only if $I = 0$ and $F = 0$. By LaSalle's invariance principle, all trajectories converge to E_0, which proves that the disease-free equilibrium is globally asymptotically stable. □

Theorem 3. *If $\mathcal{R}_0 > 1$, the endemic equilibrium E^* of system (1) exists and is globally asymptotically stable.*

Proof. Assume that $\mathcal{R}_0 > 1$ so that the endemic equilibrium $E^* = (N^*, F^*, I^*)$ exists and belongs to the interior of the positively invariant region. Consider the Lyapunov function

$$V_2(N,F,I) = N - N^* - N^* \ln\left(\frac{N}{N^*}\right) + F - F^* - F^* \ln\left(\frac{F}{F^*}\right) \quad + I - I^* - I^* \ln\left(\frac{I}{I^*}\right).$$

The function V is nonnegative for all (N, F, I) in the feasible region and satisfies $V_2(N, F, I) = 0$ if and only if $(N, F, I) = (N^*, F^*, I^*)$. Moreover, V_2 is radially unbounded in the interior of the region. Differentiating V along the trajectories of system (1) yields

$$\dot{V}_2 = \left(1 - \frac{N^*}{N}\right) \dot{\mathrm{N}} + \left(1 - \frac{F^*}{F}\right) \dot{\mathrm{F}} + \left(1 - \frac{I^*}{I}\right) \dot{I}.$$

Substituting the right-hand sides of the system and using the equilibrium relations satisfied at E^*, namely

$$\alpha_1 F^* + \alpha_2(T^*) I^* = 0, \qquad \beta_1(T^*) I^*(1 - F^*) = \mu F^*, \qquad \eta H + \kappa F^* = \delta(T^*) I^*,$$

we obtain after simplification

$$\dot{V}_2 = -\alpha_1 (F - F^*)^2 - \alpha_2(T^*)(I - I^*)^2 - \mu \frac{(F - F^*)^2}{F} - \delta(T^*) \frac{(I - I^*)^2}{I} \leq 0.$$

Hence, $\dot{V}_2$ is negative semi-definite in the feasible region and $\dot{V}_2 = 0$ if and only if $N = N^*$, $F = F^*$ and $I = I^*$. Therefore, the largest invariant set contained in $\{(N, F, I) : \dot{V}_2 = 0\}$ is the singleton $\{E^*\}$. By LaSalle's invariance principle, every solution of system (1) starting in the feasible region converges to the endemic equilibrium E^* as $t \to \infty$. This proves that E^* is globally asymptotically stable. □

4 Stochastic Switching Model

4.1 Existence, Uniqueness, and Positivity of Solutions

Theorem 4. *For any initial condition* $(N(0), F(0), I(0), G(0), T(0)) \in \mathbb{R}^5_+$, $r(0) \in \mathcal{M}$, *system* (2) *admits a unique global solution* $(N(t), F(t), I(t), G(t), T(t), r(t))$, $t \geq 0$, *which remains positive almost surely. In particular,* $N(t)$, $F(t)$, $I(t)$, $G(t)$, $T(t) > 0$ *for all* $t \geq 0$ *a.s.*

Proof. The proof is carried out in three steps.

Step 1: Local Existence and Uniqueness. For a fixed regime $r(t) = i \in \mathcal{M}$, system (2) reduces to a classical stochastic differential equation in $\mathbb{R}^5_+$. Let

$$X(t) = (N(t), F(t), I(t), G(t), T(t))^\top.$$

For each $i \in \mathcal{M}$, the drift and diffusion coefficients of the system are locally Lipschitz continuous with respect to X and satisfy the linear growth condition, since they are composed of linear and bilinear functions of the state variables. Therefore, by the classical existence and uniqueness theorem for stochastic differential equations (see [?]), there exists a unique local solution defined on the interval $[0, \tau_e)$, where τ_e denotes the explosion time.

Step 2: Global Existence (Non-explosion). To prove that the solution is global, we introduce the Lyapunov function

$$L_1(X) = N + F + I + G + T.$$

Applying Itô's formula to $V(X(t))$ gives

$$dL_1(t) = \mathcal{L}L_1(X(t), r(t))\, dt + \sum_{j=1}^{5} \sigma_j^{r(t)} X_j(t)\, dB_j(t),$$

where $\mathcal{L}$ denotes the infinitesimal generator of the stochastic system.
Using the structure of the model equations, it follows that there exists a constant $K > 0$ such that

$$\mathcal{L}L_1(X(t), r(t)) \leq K\big(1 + L_1(t)\big).$$

Define the stopping time

$$\tau_n = \inf\{t \geq 0 : L_1(t) \geq n\}.$$

Taking expectations and applying Gronwall's inequality yields

$$\mathbb{E}\big[L_1(t \wedge \tau_n)\big] \leq (L_1(0) + Kt)e^{Kt}.$$

Letting $n \to \infty$ implies that $\tau_e = \infty$ almost surely. Consequently, the solution exists globally for all $t \geq 0$.

Step 3: Positivity of Solutions. To establish the positivity of the solution, we apply Itô's formula to the logarithmic transformation of each state variable. For instance, for $N(t)$ we obtain

$$d\ln N(t) = \Big[-\alpha_1^{r(t)} F(t) - \alpha_2^{r(t)} T(t) I(t) - \tfrac{(\sigma_1^{r(t)})^2}{2} \Big] dt + \sigma_1^{r(t)} dB_1(t).$$

Since the stochastic differential equation for $\ln N(t)$ admits a finite solution for all $t \geq 0$, it follows that $N(t) > 0$ almost surely. By applying the same argument to the remaining variables $F(t)$, $I(t)$, $G(t)$, and $T(t)$, we conclude that all state variables remain strictly positive with probability one. Combining the results of the above steps completes the proof.

4.2 Almost Sure Extinction

We investigate sufficient conditions under which the fibrosis and inflammation compartments $F(t)$ and $I(t)$ of system (2) become extinct almost surely.

Theorem 5 (Almost sure extinction). *Let $r(t)$ be an irreducible continuous-time Markov chain with state space $\mathcal{M} = \{1, \dots, m\}$ and stationary distribution $\pi = (\pi_1, \dots, \pi_m)$. Assume that there exist positive constants a_i and b_i such that, for each regime $i \in \mathcal{M}$, the drift of the (F, I) subsystem satisfies*

$$\frac{d}{dt}\big(\ln F(t) + \ln I(t)\big) \le a_i - b_i - \frac{1}{2}\big((\sigma_2^i)^2 + (\sigma_3^i)^2\big).$$

Define the stochastic threshold

$$\mathcal{R}_s = \sum_{i \in \mathcal{M}} \pi_i \frac{a_i}{b_i} - \frac{1}{2} \sum_{i \in \mathcal{M}} \pi_i \big((\sigma_2^i)^2 + (\sigma_3^i)^2\big).$$

If $\mathcal{R}_s < 1$, then

$$\lim_{t \to \infty} F(t) = 0, \qquad \lim_{t \to \infty} I(t) = 0 \quad \textit{almost surely.}$$

Proof. Consider the Lyapunov function

$$L_2(t) = \ln F(t) + \ln I(t),$$

which is well defined for all $t \ge 0$ since $F(t), I(t) > 0$ almost surely. Applying Itô's formula to $V(t)$ yields

$$\begin{aligned} dL_2(t) = &\left[\frac{\beta_1^{r(t)}(T) I(t)(1 - F(t))}{F(t)} - \mu^{r(t)} + \frac{\eta^{r(t)} H + \kappa^{r(t)} F(t)}{I(t)} - \delta^{r(t)}(T) \right] dt \\ &- \frac{1}{2}\big((\sigma_2^{r(t)})^2 + (\sigma_3^{r(t)})^2\big) dt + \sigma_2^{r(t)}\, dB_2(t) + \sigma_3^{r(t)}\, dB_3(t). \end{aligned}$$

Since $0 < F(t) \le 1$ and all parameters are positive, there exist constants $a_{r(t)} > 0$ and $b_{r(t)} > 0$ such that

$$dL_2(t) \le \left[a_{r(t)} - b_{r(t)} - \frac{1}{2}\big((\sigma_2^{r(t)})^2 + (\sigma_3^{r(t)})^2\big) \right] dt + \sigma_2^{r(t)}\, dB_2(t) + \sigma_3^{r(t)}\, dB_3(t).$$

Integrating both sides from 0 to t and dividing by t gives

$$\frac{L_2(t) - L_2(0)}{t} \le \frac{1}{t} \int_0^t \left[a_{r(s)} - b_{r(s)} - \frac{1}{2}\big((\sigma_2^{r(s)})^2 + (\sigma_3^{r(s)})^2\big) \right] ds + \frac{M(t)}{t},$$

where $M(t)$ is a local martingale. Since the Markov chain $r(t)$ is ergodic with stationary distribution π, the ergodic theorem implies

$$\lim_{t \to \infty} \frac{1}{t} \int_0^t \left[a_{r(s)} - b_{r(s)} - \frac{1}{2}\big((\sigma_2^{r(s)})^2 + (\sigma_3^{r(s)})^2\big) \right] ds = \sum_{i \in \mathcal{M}} \pi_i \left(a_i - b_i - \frac{1}{2}\big((\sigma_2^i)^2 + (\sigma_3^i)^2\big) \right).$$

Moreover, by the strong law of large numbers for local martingales,

$$\lim_{t \to \infty} \frac{M(t)}{t} = 0 \quad \text{almost surely.}$$

Therefore,

$$\limsup_{t\to\infty} \frac{L_2(t)}{t} \le \sum_{i\in\mathcal{M}} \pi_i \left(a_i - b_i - \frac{1}{2}\big((\sigma_2^i)^2 + (\sigma_3^i)^2\big) \right).$$

If $\mathcal{R}_s < 1$, the right-hand side is negative, which implies $\lim_{t\to\infty} L_2(t) = -\infty$ almost surely.
Consequently,

$$\lim_{t\to\infty} F(t) = 0, \qquad \lim_{t\to\infty} I(t) = 0 \quad \text{almost surely.}$$

4.3 Persistence in Mean

We establish conditions ensuring that the fibrosis and inflammation compartments persist on average. In stochastic epidemic models, persistence in mean describes the situation where the long–term time averages of the state variables remain strictly positive.

Theorem 6. *Assume that the Markov chain $r(t)$ is irreducible with stationary distribution*
$\pi = (\pi_1, \ldots, \pi_m)$ *and that the stochastic threshold satisfies $\mathcal{R}_s > 1$. Then the fibrosis and inflammation populations of system (2) are persistent in mean, that is,*

$$\liminf_{t\to\infty} \frac{1}{t}\int_0^t F(s)\,ds > 0, \qquad \liminf_{t\to\infty} \frac{1}{t}\int_0^t I(s)\,ds > 0 \quad \textit{almost surely.}$$

Proof. Consider the stochastic Lyapunov function

$$L_3(t) = \ln F(t) + \ln I(t),$$

which is well defined since $F(t), I(t) > 0$ almost surely.
Applying Itô's formula yields

$$dL_3(t) = \frac{1}{F(t)}\,dF(t) + \frac{1}{I(t)}\,dI(t) - \frac{1}{2}\frac{(dF(t))^2}{F(t)^2} - \frac{1}{2}\frac{(dI(t))^2}{I(t)^2}.$$

Substituting the stochastic equations for $F(t)$ and $I(t)$ from system (??), we obtain

$$dL_3(t) = \left[\frac{\beta_1^{r(t)}(T)I(t)(1-F(t))}{F(t)} - \mu^{r(t)} + \frac{\eta^{r(t)}H + \kappa^{r(t)}F(t)}{I(t)} - \delta^{r(t)}(T) \right] dt$$
$$- \frac{1}{2}\big((\sigma_2^{r(t)})^2 + (\sigma_3^{r(t)})^2\big)dt + \sigma_2^{r(t)}\,dB_2(t) + \sigma_3^{r(t)}\,dB_3(t).$$

Since $0 < F(t) \le 1$ and all parameters are positive, there exist constants $a_{r(t)} > 0$ and $b_{r(t)} > 0$ such that

$$\frac{\beta_1^{r(t)}(T)I(t)(1-F(t))}{F(t)} + \frac{\eta^{r(t)}H + \kappa^{r(t)}F(t)}{I(t)} \ge a_{r(t)},$$

and

$$\mu^{r(t)} + \delta^{r(t)}(T) \leq b_{r(t)}.$$

Consequently,

$$dL_3(t) \geq \left[a_{r(t)} - b_{r(t)} - \frac{1}{2}\big((\sigma_2^{r(t)})^2 + (\sigma_3^{r(t)})^2\big)\right] dt + \sigma_2^{r(t)}\, dB_2(t) + \sigma_3^{r(t)}\, dB_3(t).$$

Integrating from 0 to t gives

$$L_3(t) - L_3(0) \geq \int_0^t \left[a_{r(s)} - b_{r(s)} - \frac{1}{2}\big((\sigma_2^{r(s)})^2 + (\sigma_3^{r(s)})^2\big)\right] ds + M(t),$$

where

$$M(t) = \int_0^t \sigma_2^{r(s)}\, dB_2(s) + \int_0^t \sigma_3^{r(s)}\, dB_3(s)$$

is a local martingale. Dividing by t and taking the limit inferior yields

$$\frac{L_3(t)}{t} \geq \frac{1}{t}\int_0^t \left[a_{r(s)} - b_{r(s)} - \frac{1}{2}\big((\sigma_2^{r(s)})^2 + (\sigma_3^{r(s)})^2\big)\right] ds + \frac{M(t)}{t}.$$

Since $r(t)$ is ergodic, the ergodic theorem implies

$$\lim_{t\to\infty} \frac{1}{t}\int_0^t \left[a_{r(s)} - b_{r(s)} - \frac{1}{2}((\sigma_2^{r(s)})^2 + (\sigma_3^{r(s)})^2)\right] ds = \sum_{i\in\mathcal{M}} \pi_i \left(a_i - b_i - \frac{1}{2}((\sigma_2^i)^2 + (\sigma_3^i)^2)\right).$$

Moreover, by the strong law of large numbers for martingales, we have $\lim_{t\to\infty} \dfrac{M(t)}{t} = 0$ almost surely. Hence,

$$\liminf_{t\to\infty} \frac{L_3(t)}{t} \geq \sum_{i\in\mathcal{M}} \pi_i \left(a_i - b_i - \frac{1}{2}((\sigma_2^i)^2 + (\sigma_3^i)^2)\right).$$

If $\mathcal{R}_s > 1$, the right-hand side is positive. Therefore,

$$\liminf_{t\to\infty} \frac{1}{t}\int_0^t \ln(F(s)I(s))\, ds > 0.$$

Using Jensen's inequality, it follows that

$$\liminf_{t\to\infty} \frac{1}{t}\int_0^t F(s)\, ds > 0, \qquad \liminf_{t\to\infty} \frac{1}{t}\int_0^t I(s)\, ds > 0 \quad \text{almost surely.}$$

Thus, the fibrosis and inflammation populations persist in mean.

5 Numerical Simulations

5.1 Numerical Methodology and Data-Driven Framework

Before performing parameter estimation and simulations, we briefly describe the numerical methods used to solve both the deterministic and stochastic versions of the proposed CKD model. This step ensures the stability and reliability of the computational results. Model parameters are then estimated from clinical data, and the calibrated model is used to investigate disease progression and treatment effects. Numerical simulations are performed to illustrate the theoretical findings and to analyze the qualitative dynamics of the renal compartments under treatment and stochastic perturbations, using biologically realistic parameter values consistent with clinical observations reported in the literature.

5.2 Numerical Scheme for the Stochastic CKD Model

To approximate the solution of the stochastic CKD model, we employ the Euler–Maruyama scheme with Milstein correction, which is well suited for stochastic differential equations with multiplicative noise and preserves the positivity of state variables. Let $\Delta t > 0$ denote the time step and let $\zeta_{k,i} \sim \mathcal{N}(0,1)$, $k = 1, \ldots, 5$, be independent standard Gaussian random variables.

For simplicity of numerical implementation, we first consider system (2) without regime switching. The discretized scheme is given by

$$N_{i+1} = N_i + \Big[-\alpha_1 F_i N_i - \alpha_2(T_i) I_i N_i \Big] \Delta t + \sigma_1 N_i \sqrt{\Delta t}\, \zeta_{1,i} + \frac{\sigma_1^2}{2} N_i (\zeta_{1,i}^2 - 1) \Delta t,$$

$$F_{i+1} = F_i + \Big[\beta_1(T_i) I_i (1 - F_i) - \mu F_i \Big] \Delta t + \sigma_2 F_i \sqrt{\Delta t}\, \zeta_{2,i} + \frac{\sigma_2^2}{2} F_i (\zeta_{2,i}^2 - 1) \Delta t,$$

$$I_{i+1} = I_i + \Big[\eta H + \kappa F_i - \delta(T_i) I_i \Big] \Delta t + \sigma_3 I_i \sqrt{\Delta t}\, \zeta_{3,i} + \frac{\sigma_3^2}{2} I_i (\zeta_{3,i}^2 - 1) \Delta t,$$

$$G_{i+1} = G_i + \Big[\rho N_i - \gamma F_i G_i \Big] \Delta t + \sigma_4 G_i \sqrt{\Delta t}\, \zeta_{4,i} + \frac{\sigma_4^2}{2} G_i (\zeta_{4,i}^2 - 1) \Delta t,$$

$$T_{i+1} = T_i + \Big[u(t_i) - \omega T_i \Big] \Delta t + \sigma_5 T_i \sqrt{\Delta t}\, \zeta_{5,i} + \frac{\sigma_5^2}{2} T_i (\zeta_{5,i}^2 - 1) \Delta t.$$

Here, $N(t)$ denotes the functional nephron population, $F(t)$ the level of fibrosis, $I(t)$ the inflammatory activity, $G(t)$ the glomerular damage, and $T(t)$ the treatment intensity. The parameters $\sigma_k > 0$, $k = 1, \ldots, 5$, represent the intensities of environmental and physiological stochastic fluctuations affecting each compartment. This numerical framework preserves the biological feasibility of the solutions and enables the investigation of extinction, persistence, and long-term stochastic behavior of CKD progression under different treatment strategies.

5.3 Clinical Dataset and Data-Driven Calibration

5.3.1 Clinical Dataset

The clinical data used in this study were obtained from the *Chronic Kidney Disease (CKD) Dataset* available in the UCI Machine Learning Repository [20], which contains medical records of approximately 400 patients. The dataset includes demographic, clinical, and laboratory variables relevant to renal function assessment and CKD progression, such as age, blood pressure, serum creatinine, blood urea, hemoglobin level, albumin, sugar, and the estimated glomerular filtration rate (eGFR), commonly used as a proxy for kidney function. Additional categorical indicators, including hypertension and diabetes status, are also provided. Prior to model calibration, the dataset was preprocessed to ensure data quality and numerical consistency. Missing values were handled using standard imputation methods (mean substitution for continuous variables and mode substitution for categorical variables). Continuous variables were subsequently normalized to reduce scale effects and facilitate the parameter estimation procedure.

5.3.2 Estimated Parameters

Using this calibration procedure, a subset of key model parameters was estimated from the dataset, while the remaining parameters were fixed based on biological relevance and consistency with the literature. The resulting parameter values used in the simulations are summarized in Table 2. Several parameters were fixed to avoid identifiability issues and ensure biological plausibility. In particular, μ represents the natural fibrosis resolution rate and was set to $\mu = 0.05$, reflecting the slow regression of fibrosis in CKD. The feedback coefficient $\kappa = 0.03$ accounts for the reinforcing interaction between fibrosis and inflammation. The parameter $\rho = 1$ normalizes the contribution of functional nephrons to the glomerular filtration rate. The glomerular damage coefficient was defined as $\gamma = |\alpha_1| + |\alpha_2|$ to capture the cumulative effects of fibrosis and inflammation. Finally, the treatment decay rate was fixed at $\omega = 0.1$, consistent with typical pharmacodynamic assumptions. The validation root mean square error (RMSE) obtained for the renal function proxy was 0.4159, indicating good agreement between model predictions and clinical observations and confirming the ability of the proposed CKD model to capture the overall dynamics of renal function.

Table 2. Estimated and fixed model parameters for the CKD model

Parameter	Description	Value
α_1	Nephron loss induced by fibrosis	0.0334
α_2	Nephron loss induced by inflammation	0.0465
β_1	Fibrosis activation rate	0.3037
δ	Inflammation clearance rate	0.9252
η	External inflammatory stimulus	0.0447
μ	Natural fibrosis resolution rate	0.05 (fixed)
κ	Fibrosis–inflammation feedback	0.03 (fixed)
ρ	Nephron contribution to GFR	1.0 (fixed)
γ	Glomerular damage coefficient	$\lvert\alpha_1\rvert + \lvert\alpha_2\rvert$
ω	Treatment decay rate	0.1 (fixed)

5.4 Graphical Validation and Numerical Simulations

After the quantitative validation of the proposed CKD model using the Root Mean Square Error (RMSE), graphical numerical simulations are performed to further assess the qualitative behavior of the system. While the RMSE provides a numerical measure of the agreement between model predictions and clinical data, graphical simulations allow a deeper interpretation of the temporal evolution of key biological compartments and the impact of stochastic perturbations and treatment strategies. In particular, the time evolution of fibrosis $F(t)$, inflammation $I(t)$, renal function proxy $G(t)$, and treatment intensity $T(t)$ is illustrated under both deterministic and stochastic formulations of the model. The comparison between deterministic and stochastic trajectories highlights the role of environmental and physiological noise in disease progression and treatment response. These simulations confirm that the stochastic model remains biologically consistent and numerically stable, in agreement with the theoretical results on positivity, persistence, and long-term behavior. Moreover, the graphical results complement the RMSE-based validation by showing that the estimated parameters lead to realistic disease dynamics over time. In particular, the renal function trajectory $G(t)$ exhibits smooth degradation patterns modulated by treatment effects, while fibrosis and inflammation remain within biologically plausible ranges. This combined quantitative–qualitative validation strengthens the reliability of the proposed CKD model for predictive and exploratory studies.

5.5 Biological Interpretation of Numerical Simulations

Figure 1 presents the temporal evolution of the main renal compartments of the CKD model, namely the functional nephron population $N(t)$, fibrosis level $F(t)$, inflammatory activity $I(t)$, renal function proxy $G(t)$, and treatment intensity $T(t)$, for both deterministic and stochastic formulations. These simulations illustrate the extinction and persistence properties established in the theoretical

analysis. The functional nephron population $N(t)$ gradually declines, reflecting irreversible nephron loss induced by sustained inflammation and fibrosis. In agreement with the extinction results, persistent pathological stress drives $N(t)$ toward low levels, corresponding biologically to advanced CKD stages. In contrast, the fibrosis variable $F(t)$ stabilizes at a positive level, indicating long-term persistence of fibrotic tissue. This behavior is consistent with the persistence theorem and reflects the well-known irreversibility of renal fibrosis once structural remodeling becomes established. Inflammatory activity $I(t)$ decreases significantly in the presence of treatment and may fluctuate around low values, illustrating a treatment-driven extinction tendency. Clinically, this corresponds to controlled inflammatory activity and disease stabilization. The renal function indicator $G(t)$ remains positive but progressively decreases as nephron loss and fibrosis accumulate. This persistence above zero represents partial preservation of renal function, consistent with compensated CKD dynamics. Finally, stochastic perturbations introduce variability around the deterministic trajectories without altering the qualitative long-term behavior, highlighting the influence of physiological variability and environmental factors in disease progression.

5.6 Numerical Simulations and Treatment Impact

Following model calibration, numerical simulations were conducted to analyze the impact of therapeutic intervention on CKD dynamics. Figure 2 compares the evolution of fibrosis $F(t)$, inflammation $I(t)$, and renal function $G(t)$ with and without treatment. In the absence of treatment, fibrosis and inflammation progressively increase, leading to a gradual decline in renal function. Conversely, treatment substantially reduces inflammatory activity, which slows fibrotic progression and helps maintain higher levels of renal function. These results are consistent with the theoretical extinction–persistence analysis: effective therapeutic control of inflammation can suppress pathological dynamics and delay renal deterioration. Biologically, this highlights the importance of early and sustained treatment strategies to limit fibrosis development and preserve nephron function in chronic kidney disease.

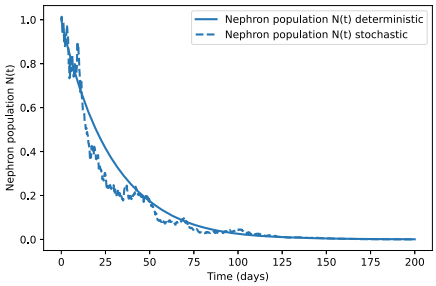

(a) $N(t)$ – Functional nephron population

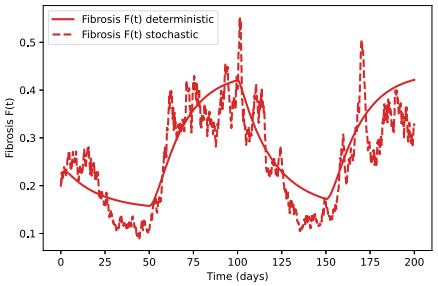

(b) $F(t)$ – Renal fibrosis

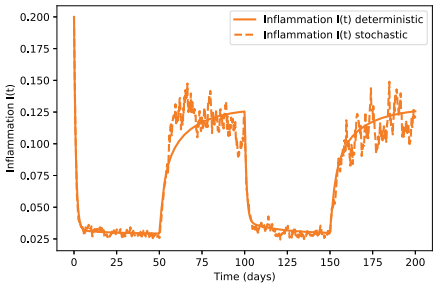

(c) $I(t)$ – Inflammatory activity

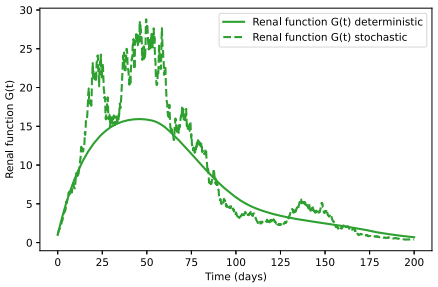

(d) $G(t)$ – Renal function (GFR proxy)

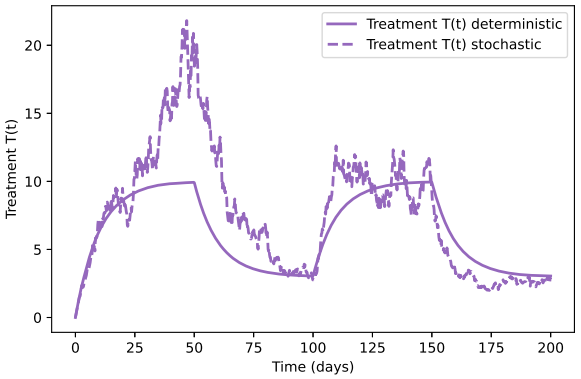

(e) $T(t)$ – Treatment intensity

Fig. 1. Numerical simulations of the CKD model showing the temporal evolution of nephron population $N(t)$, fibrosis $F(t)$, inflammation $I(t)$, renal function $G(t)$, and treatment intensity $T(t)$ for both deterministic and stochastic formulations, using the estimated parameters reported in Table 2.

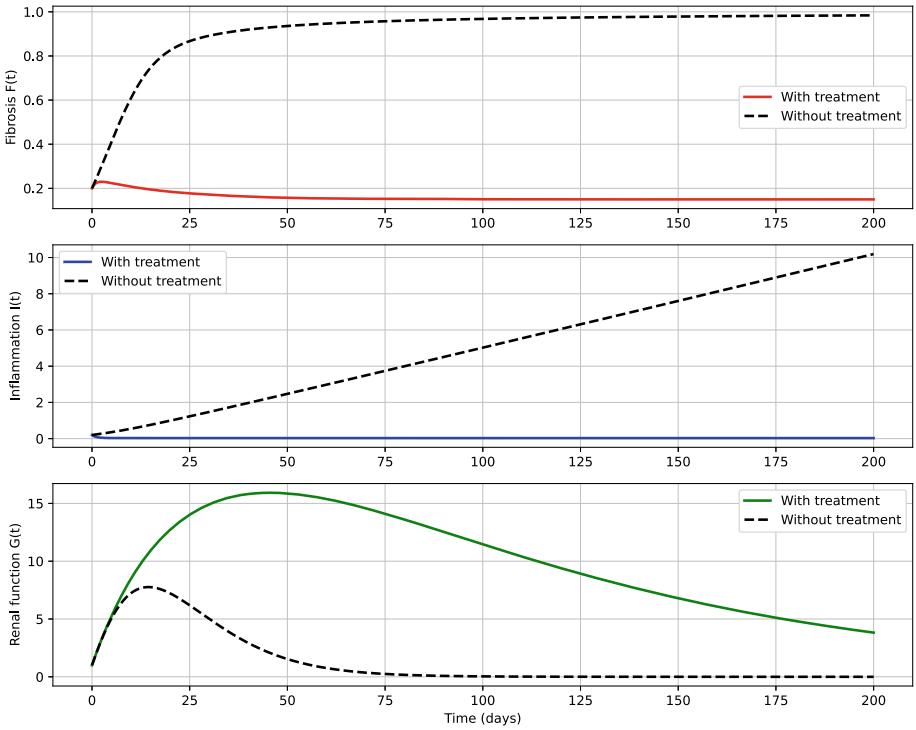

Fig. 2. Comparison of the temporal dynamics of the CKD model with and without treatment. (a) Evolution of renal fibrosis $F(t)$, (b) evolution of inflammatory activity $I(t)$, (c) evolution of renal function $G(t)$ (GFR proxy). Colored solid lines represent the treated scenario, whereas black dashed lines correspond to the absence of treatment.

6 Conclusion

In this work, we developed a mathematical framework to investigate the dynamics of chronic kidney disease (CKD) using both deterministic and stochastic modeling approaches. The proposed model incorporates key biological mechanisms involved in CKD progression, including nephron loss, fibrosis development, inflammatory activity, renal function decline, and therapeutic intervention. For the deterministic model, we established the existence and global stability of biologically relevant equilibria. The model was then extended to a stochastic formulation to account for biological variability and environmental uncertainty. Using Itô calculus and Lyapunov techniques, sufficient conditions for stochastic extinction and persistence were obtained, showing that random perturbations may significantly influence long-term disease dynamics. Model parameters were calibrated using clinical data, and numerical simulations were performed to validate the theoretical results. The simulations illustrate the impact of treatment in reducing inflammation and fibrosis while preserving renal function. Moreover, stochastic simulations highlight the role of variability in shaping disease trajec-

tories. Overall, the proposed framework provides a useful tool for understanding CKD progression and evaluating therapeutic strategies. Future work may incorporate patient heterogeneity, adaptive treatment protocols, and additional biological mechanisms to further improve the model's clinical relevance.

References

1. Kdigo clinical practice guideline for the evaluation and management of chronic kidney disease. Kidney Int. Suppl. (2013)
2. Abdelhag, M.E.: A systematic review of machine learning methods for chronic kidney disease diagnosis and prediction (2020–2025). Saudi J. Appl. Sci. Technol. **2**(1) (2026)
3. Bera, S., Khajanchi, S., Kar, T.K.: Stochastic persistence, extinction and stationary distribution in HTLV-i infection model with CTL immune response. Qual. Theory Dyn. Syst. **23**(Suppl 1), 265 (2024)
4. Boulaasair, L.: Threshold properties of a stochastic epidemic model with a variable vaccination rate. Bull. Biomath. **1**(2), 177–191 (2023)
5. Cheng, D., Wang, J., Hu, X.: An extension of Lasalle's invariance principle and its application to multi-agent consensus. IEEE Trans. Autom. Control **53**(7), 1765–1770 (2008)
6. Das, P., Upadhyay, R.K., Misra, A.K., Rihan, F.A., Das, P., Ghosh, D.: Mathematical model of covid-19 with comorbidity and controlling using non-pharmaceutical interventions and vaccination. Nonlinear Dyn. **106**(2), 1213–1227 (2021)
7. Delrue, C., De Bruyne, S., Speeckaert, M.M.: Application of machine learning in chronic kidney disease: current status and future prospects. Biomedicines **12**(3), 568 (2024)
8. Diekmann, O., Heesterbeek, J.A.P., Metz, J.A.J.: On the definition and the computation of the basic reproduction ratio r 0 in models for infectious diseases in heterogeneous populations. J. Math. Biol. **28**(4), 365–382 (1990)
9. Din, A., Amine, S., Allali, A.: A stochastically perturbed co-infection epidemic model for Covid-19 and hepatitis b virus. Nonlinear Dyn. **111**(2), 1921–1945 (2023)
10. Gogoi, P., Valan, J.A.: Machine learning approaches for predicting and diagnosing chronic kidney disease: current trends, challenges, solutions, and future directions. Int. Urol. Nephrol. **57**(4), 1245–1268 (2025)
11. Hajri, Y., Allali, A., Amine, S.: A delayed deterministic and stochastic SIRICV model: HOPF bifurcation and stochastic analysis. Math. Comput. Simul. **215**, 98–121 (2024)
12. Salle, L., J.P.: An invariance principle in the theory of stability. Technical report (1966)
13. Liu, Q., Din, A., Allali, A.: Analysis of a multiply delayed stochastic EBOLA model based on probability density function with case study. European Phy. J. Plus **138**(11), 1–18 (2023)
14. Mao, L., et al.: Knowledge-informed machine learning for cancer diagnosis and prognosis: a review. IEEE Trans. Autom. Sci. Eng. **22**, 10008–10028 (2024)
15. Mao, X.: Stochastic differential equations and applications. Elsevier (2007)
16. Mei, W., Bullo, F.: Lasalle invariance principle for discrete-time dynamical systems: a concise and self-contained tutorial. arXiv preprint arXiv:1710.03710 (2017)
17. Patharkar, A., Cai, F., Al-Hindawi, F., Wu, T.: Predictive modeling of biomedical temporal data in healthcare applications: review and future directions. Front. Physiol. **15**, 1386760 (2024)

18. Pervyshin, N.A.: Mathematical modeling of the chronic kidney disease progression rate in patients with type 2 diabetes mellitus. Sci. Innov. Med. **9**(2), 88–94 (2024)
19. Reckell, T., Sterner, B., Jevtić, P.: The basic reproduction number for petri net models: a next-generation matrix approach. Appl. Sci. **15**(23), 12827 (2025)
20. Rubini, L., Soundarapandian, P., Eswaran, P.: Chronic kidney disease dataset. https://archive.ics.uci.edu/ml/datasets/Chronic+Kidney+Disease (2015). UCI Machine Learning Repository
21. Sangeetha, T.E., Pandiyan, P., Kumar, R.H., Bose, G.S.C.: A stochastic model for chronic kidney disease. Adv. Math. Sci. J. **10**(10), 3363–3372 (2021)
22. Sharma, A., Lysenko, A., Jia, S., Boroevich, K.A., Tsunoda, T.: Advances in AI and machine learning for predictive medicine. J. Hum. Genet. **69**(10), 487–497 (2024)
23. Thomas, H.Y., Ford Versypt, A.N.: A mathematical model of glomerular fibrosis in diabetic kidney disease to predict therapeutic efficacy. Front. Pharmacol. **15**, 1481768 (2024)
24. Upadhyay, R.K., Acharya, S.: Modeling the recent outbreak of covid-19 in India and its control strategies. Nonlinear Anal. Model. Control **27**(2), 254–274 (2022)
25. Vaidya, S.R., Aeddula, N.R.: Chronic kidney disease. In: StatPearls [Internet]. StatPearls Publishing (2024)
26. ZHANG, Z., Xu, C., Jinying, T.: Lasalle's invariance principle for delay differential equations driven by α-stable processes. J. East China Normal Univ. (Natural Sci.) **2023**(4), 11 (2023)